Parametric Veiling-Glare Rendering

Sungkil Lee

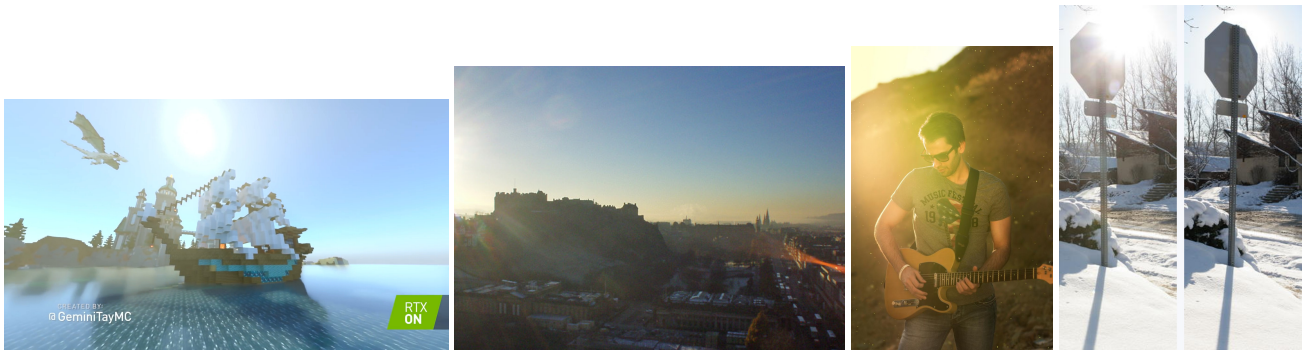

Figure 1: *Example of veiling glares (taken from wikipedia/flares) and https://www.imatest.com/docs/veilingglare/*

Abstract

To be filled later

Keywords: Lens flares, glare

1 Introduction

[TODO] Introduce approximation of boxcar superposition
[TODO] Spherical-Harmonics Approximaiton of Angular Variations
[TODO] Circular Harmonics Approximaiton of Angular Variations: https://valdes.cc/articles/ch.html

[TODO] FROM WIKIPEDIA: Veiling glare is an imperfection of performance in optical instruments (such as cameras and telescopes) arising from incoming light that strays from the normal image-forming paths, and reaches the focal plane. The effect superimposes a form of noise onto the normal image sensed by the detector (film, digital sensor, or eye viewing through an eyepiece), resulting in a final image degraded by loss of contrast and reduced definition.

Veiling glare and lens flare are effects by stray lights (ghosts) from reflections between lens barrel and sensor surfaces (see Fig. 5) [Naylor 1970]. The difference between veiling glare and lens flare is properties of ghosts. Ghosts of veiling glare have smoother edge, weaker intensity and bigger size than those of lens flare. Traditionally, these effects are not desired and regarded as an artifact in photographic and cinematographic field. But for realistic scene, they are now considered as artistic effects recently and even drawn on purpose [].

To render veiling glare and lens flare effect, some methods are suggested in the past decades. Path tracing technique [] of rays between lenses are considered as a reference solution. Higher quality have been demonstrated by results of this technique, while hundreds of hours are required to get a high-quality result.

To overcome those challenges, an approach using sparse ray tracing and rasterization is suggested by Hullin et al []. Rasterization and reduced sample size led to gain a performance of the technique, while physical properties of lenses in their model made the result retaining high quality. Later, faster method is introduced, based on flare mapping using matrices []. In comparison to the previous version, this method can produces a real-time effect, with a little loss of quality.

Decoupling flare and veiling glares are better in terms of performance. The motivation is shown in the context of HDR imaging (e.g., glare encoding [Rouf et al. 2011]). We also separate the rendering of main flares and veiling glares, and veiling glares rendered in parametric forms, speeding up rendering drastically.

In our paper, we suggest a parametric model of veiling glare. As a result, we could render a veiling glare effect can be rendered efficiently, and animation with moving a light source and a camera.

More precisely, the contributions of our paper are as follows:

- low-frequency Fourier-series approximations of glare spread functions

2 Related Work

Glare-aware photography [Raskar et al. 2008]

2.1 Removing Glares and Flares

Veiling glare removal [Talvala et al. 2007]
Removing image artifacts [Gu et al. 2009]
Geometry by deflaring [Koreban and Schechner 2009]
occlusion mask [Cozzi et al. 2018]
paraxial approximation [Smith 1971]

3 Glare Spread Function

Glare Spread Function (GSF): ISO definition
shift-invariant GSF === can be treated as PSF

GSF = (glare illuminance)/(total flux in the image of the source) [Williams 1998]

4 Model

[SLEE] MAIN IDEA: FOURIER SERIES, BUT WITH PERIODS GREATER THAN SCREEN SIZE; THEN, WE DO NOT SEE THE PERIODICITY

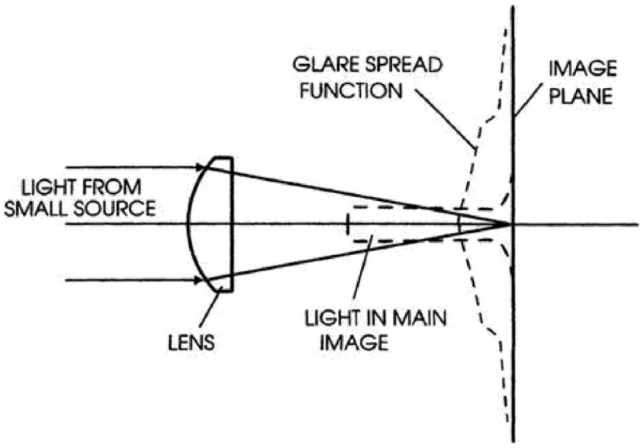

Figure 2: *The concept of glare spread function*

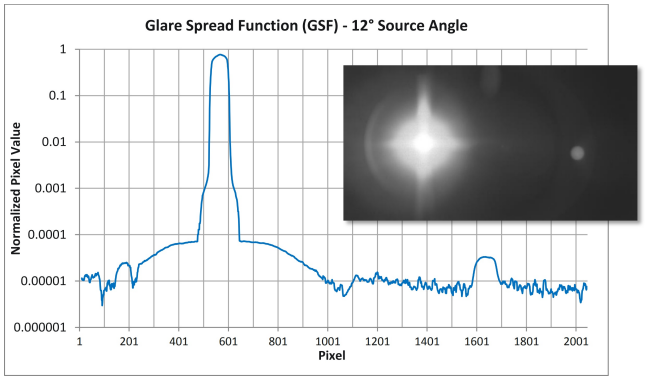

Figure 3: *GSF Example.*

A picture goes here

Figure 4: *[TODO] Draw an example of 2D glares (i.e., superposition of 2D circles).*

[TODO] It is possible to approximate H, such as Taylor expansions of logistic functions or bump functions, but its quality is significantly degraded with large distance from the center point.

4.1 1D Fourier Series Expansion

Our key idea is to assume the point-spread function (PSF) of a glare is *periodic*. Let the period be λ. Then,

$$f(x) = f(x+\lambda). \tag{1}$$

λ is *two times* of the larger dimension of the screen resolution. In this case, we only see a single instance of a glare PSF, without seeing other repeating tails. It is important T should be chosen as identical for all f_k, and this allows us to derive the aggregation of different ghosts into a unified Fourier series.

For brevity, we first define shorthands as follows:

$$c_n(x) := \cos(n\omega x) \tag{2}$$
$$s_n(x) := \sin(n\omega x), \tag{3}$$

where an angular frequency $\omega = 2\pi/\lambda$.

We assume the glare PSF is an even function; in many cases, it can be radially symmetric, but needs not to be necessarily be true. We can now use Fourier series expansion of the even function, which is truncated up to degrees N as:

$$f(x) = \sum_{n=0}^{N} a_n c_n(x), \tag{4}$$

where $N \to \infty$ converges to a true solution. From the general formula of the Fourier series expansion,

$$a_n = \frac{\tau}{\lambda}\int_{-\lambda}^{\lambda} f(x)c_n(x)dx, \tag{5}$$

where $\tau = 1$ if $n = 0$, otherwise $\tau = 2$.

4.2 2D Extension of PSFs

[TODO] Note that the summations are separable.

The previous formulation is only applicable to 1D profile. Now, we need to extend them to 2D profile for object k. It is still possible to 1D profile extend along the optical axis.

For 2D, we still assume using the same period T, and then, the periodicity satisfies:

$$f(x,y) = f(x+\lambda,y) = f(x,y+\lambda) = f(x+\lambda,y+\lambda). \tag{6}$$

Then, 2D expansion can be:

$$f(x,y) = \sum_{n=0}^{N}\sum_{m=0}^{M} g_{n,m}(x,y), \tag{7}$$

where

$$g_{n,m}(x,y) = a_{n,m}c_n(x)c_m(y) + b_{n,m}s_n(x)s_m(y). \tag{8}$$

The coefficients are found with:

$$a_{n,m} = \frac{\kappa}{\lambda^2}\int_{\lambda}\int_{\lambda} f(x,y)c_n(x)c_m(y)dxdy \tag{9}$$
$$b_{n,m} = \frac{\kappa}{\lambda^2}\int_{\lambda}\int_{\lambda} f(x,y)s_n(x)s_m(y)dxdy \tag{10}$$

where

$$\kappa = 1 \text{ if } n = 0 \text{ and } m = 0 \tag{11}$$
$$= 2 \text{ if } n = 0 \text{ or } m = 0 \tag{12}$$
$$= 4 \text{ if } n > 0 \text{ and } m > 0 \tag{13}$$

Translation When a translation exists, we can expand as:

$$g_{n,m}(x-\alpha,y-\beta) = a_{n,m}c_n(x-\alpha)c_m(y-\beta) \tag{14}$$
$$+ b_{n,m}s_n(x-\alpha)s_m(y-\beta) \tag{15}$$

by applying the theorem,

$$c(\alpha-\beta) = c(\alpha)c(\beta) + s(\alpha)s(\beta) \tag{16}$$
$$s(\alpha-\beta) = s(\alpha)c(\beta) - c(\alpha)s(\beta), \tag{17}$$

we can easily expand g.

4.3 General Glare Spread Function

Then, the entire veiling glare can be represented as an aggregation of all the functions in a set of objects K. We consider a ghost k, whose function is f_k and displaced by $\mathbf{p}_k := (x_k, y_k)$.

where

$$G_{n,m}(x,y) = A_{n,m}c_n(x)c_m(y) + B_{n,m}c_n(x)s_m(y) \tag{18}$$
$$+ C_{n,m}s_n(x)c_m(y) + D_{n,m}s_n(x)s_m(y), \tag{19}$$

where

$$A_{n,m} = \sum_{k\in K} a_{k,n,m}c_n(x_k)c_m(y_k) + b_{k,n,m}s_n(x_k)s_m(y_k), \tag{20}$$
$$B_{n,m} = \sum_{k\in K} a_{k,n,m}c_n(x_k)s_m(y_k) - b_{k,n,m}s_n(x_k)c_m(y_k), \tag{21}$$
$$C_{n,m} = \sum_{k\in K} a_{k,n,m}s_n(x_k)c_m(y_k) - b_{k,n,m}c_n(x_k)s_m(y_k), \tag{22}$$
$$D_{n,m} = \sum_{k\in K} a_{k,n,m}s_n(x_k)s_m(y_k) + b_{k,n,m}c_n(x_k)c_m(y_k). \tag{23}$$

where the coefficients are found with:

$$a_{k,n,m} = \frac{\kappa}{\lambda^2}\int_\lambda\int_\lambda f_k(x,y)c_n(x)c_m(y)dxdy \tag{24}$$
$$b_{k,n,m} = \frac{\kappa}{\lambda^2}\int_\lambda\int_\lambda f_k(x,y)s_n(x)s_m(y)dxdy \tag{25}$$

Then, $A_{n,m}$, $B_{n,m}$, $C_{n,m}$, and $D_{n,m}$ are not the functions of (x,y), and thus, we can pre-compute before pixel-wise processing. Then, this leads to a constant number of evaluation, regardless of the number of ghosts $|K|$, and only depending on N and M, which determines the precision of approximation.

The time complexity is $O(NMK)$, but we can avoid the pixel-dependent complexity. We can control the quality of approximation using N; as N increases, the quality becomes better.

4.4 Separability

[TODO] IMPORTANT

The Fourier Series can be expressed in the separable form

$$\begin{aligned} F(x,y) &= \sum_{n=0}^{N}\sum_{m=0}^{M} G_{n,m}(x,y) \\ &= \sum_{n=0}^{N}\sum_{m=0}^{M} \{A_{n,m}c_n(x)c_m(y) + B_{n,m}c_n(x)s_m(y) \\ &+ C_{n,m}s_n(x)c_m(y) + D_{n,m}s_n(x)s_m(y)\} \end{aligned} \tag{26}$$

$$\begin{aligned} \sum_{n=0}^{N}\sum_{m=0}^{M} A_{n,m}c_n(x)c_m(y) &= \sum_{n=0}^{N} c_n(x)\sum_{m=0}^{M} A_{n,m}c_m(y) \\ &= \sum_{n=0}^{N} c_n(x)A_{n,M} \end{aligned} \tag{27}$$

where

$$A_{n,M} = \sum_{m=0}^{M} A_{n,m}c_m(y) \tag{28}$$

First, fourier series coefficients are computed along coefficients' m-axis, and then computed along each column of this intermediate result. It shows that fourier series coefficients can be computed independently.

4.5 De-ringing with σ-approximation

In mathematics, σ-approximation adjusts a Fourier summation to greatly reduce the Gibbs phenomenon, which would otherwise occur at discontinuities. A σ-approximated summation for a series of period T can be written as follows :

$$s(\theta) = \frac{1}{2}a_0 + \sum_{k=1}^{m-1} sinc(\frac{k}{m})[a_k cos(\frac{2k\pi\theta}{T}) + b_k sin(\frac{2k\pi\theta}{T})] \tag{29}$$

So, in

$$F(x,y) = \sum_{n=0}^{N}\sum_{m=0}^{M} G_{n,m}(x,y) \tag{30}$$

Let's multiply sinc value

$$F_1(x,y) = \sum_{n=1}^{N}\sum_{m=0}^{M} sinc(\frac{n}{k})G_{n,m}(x,y) \tag{31}$$

where k is order(terms) of Fourier series.

4.6 Positive-valued 2D Extension of PSFs

In mathematics, σ-approximation adjusts a Fourier summation to greatly reduce the Gibbs phenomenon, which would otherwise occur at discontinuities. A σ-approximated summation for a series of period T can be written as follows :

$$s(\theta) = \frac{1}{2}a_0 + \sum_{k=1}^{m-1} sinc(\frac{k}{m})[a_k cos(\frac{2k\pi\theta}{T}) + b_k sin(\frac{2k\pi\theta}{T})] \tag{32}$$

So, in

$$f(x,y) = \sum_{n=0}^{N}\sum_{m=0}^{M} G_{n,m}(x,y), \tag{33}$$

Let's multiply sinc value

$$F(x,y) = \sum_{n=1}^{N}\sum_{m=1}^{M} sinc(\frac{n}{N})sinc(\frac{m}{M})G_{n,m}(x,y) \tag{34}$$

With this process, we can remove de-ringing artifact.

[TODO] The boundary conditions applied to the heat equation are called 'Dirichlet boundary conditions When we draw u(x, y) on [a, b]x[c, d], we have to check u(x, c) u(x, d) u(a, y) u(b, y) If all of those four values are zero, which means the values of the function on the boundary of the rectangle are zero, we can reduce consine terms (have to prove whether f(x, y) satisfies Dirichlet boundary conditions.)

If function F satisfies Dirichlet conditions, F is equal to the sum of its Fourier Series at each continuos points. We have to check : 1) F is absolutely integrable and BV function in any bounded interval. 2) F have finite number of discontinuities.

Since we suppose that periods of fourier sum is greater than screen size, the screen itself is bounded interval of the given function.

// stackexchange

$$C_{n,m} = \frac{\int_0^b \int_0^a f(x,y) s(\frac{nx\pi}{a}) s(\frac{mx\pi}{b}) dxdy}{\int_0^b \int_0^a s^2(\frac{2nx\pi}{a}) s^2(\frac{2mx\pi}{b}} \tag{35}$$

Since

$$\begin{aligned} &\int_0^b \int_0^a f(x,y) sin^2(\frac{nx\pi}{a}) sin^2(\frac{mx\pi}{b}) \\ &= \int_0^a \frac{1-cos(\frac{2nx\pi}{a})}{2} \int_0^b \frac{1-cos(\frac{2nx\pi}{a})}{2} \\ &= \frac{ab}{4} \end{aligned} \tag{36}$$

$$C_{n,m} = \frac{4}{ab} \int_0^b \int_0^a f(x,y) s(\frac{nx\pi}{a}) s(\frac{mx\pi}{b}) dxdy \tag{37}$$

5 Glare Model

[TODO] Say f is a radially symmetric function; typical example is a disk, but we can apply others such as cosine

5.1 Square Waves

Veiling glare can be interpreted as a superposed response of weak and (potentially large) ghosts in optical systems (see Fig. 4). Assuming each ghost k is a 2D circle with constant intensity I_k, it cross-section through the center line can be represented as the superpositions of boxcar functions (see Fig. 6).

5.1.1 Boxcar Functions

For simplicity, first suppose a 1D intensity function of a ghost, which has a intensity I only in $[-r,r]$ and 0 in others. Then, the intensity can be represented as a symmetric boxcar function:

$$f(x) = I(H(t+r) - H(t-r)), \tag{38}$$

where I is the constant intensity profile of a ghost k, and H is the Heaviside step function.

Since the veiling glare can be dynamic along the camera's movements, its temporal interpolation is crucial for effective representation. However, H is not differentiable, and is not appropriate for this purpose.

$$a_n = \frac{2I}{\lambda} \int_{-r}^{r} c_n(x) dx = \frac{4I}{n\omega\lambda} s_n(r), \text{where } n > 0 \tag{39}$$

$$= \frac{2Ir}{\lambda}, \text{where } n = 0 \tag{40}$$

5.2 Global Rotation

Rotate the function globally.

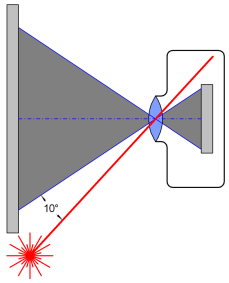

Figure 5: *Glare from stray lights. As shown in the figure, a stray light can still reveal glare.*

5.3 Angular Parameter Control and 3D LUT for Temporal Animation

One good thing is we only use the coefficients to represent the functions, and that means, we may temporal regression to represent them.

Actually, once we have angle-dependent parameter derivation, then temporal animation is likely to be trivial.

Build 3D LUT for animation: z: angular deviation

5.4 Time-Complexity Analysis

show pass-by-pass complexity, and compare with straightforward approach and object-wise repetition

5.5 Stray Light

We can still consider stray light, because we use analytic control.

6 Parallel Aggregation on GPU

To obtain high-quality approximation without marginal ringing, we need high degrees of approximation for example thousands of glares.

It is non-trivial for CPU, but we do accelerate this step in GPU, which allows quickly evaluate up to very high degrees (e.g., 4096). It takes only less than 1 ms.

6.1 a(r) can use offline LUT processing

A needs to be online processing to reflect c_k and $a(r)$

7 Acceleration with Sequential LUTs

Here, we present how to separately evaluate the functions, offline preprocessing, run-time preprocessing, and run-time pixel processing.

7.1 Offline: Shape-Invariant Functions; Size Only Dependent a, b

Periodicity leads to $a_{k,n,m}$ do not have to be re-evaluated for the movement of ghosts, as long as the shape stays constant.

[TODO] Same function only size changes: We can build a look-up table for $a_{k,n,m}$ to $a_{n,m}(r)$ depending on only the size. We can

compute this offline only once. By this way, we can apply any shapes of apertures.

Baking Diffractions Diffractions can be pre-baked as a look-up table, which may play a significant role for dynamics.

7.2 Online: Object Constant Evaluation

Pre-compute online,
and store into uniform buffer.

7.3 Online: 2-Pass Pixel-Wise Separable Evaluation

7.4 Complete LUT for the entire pipeline

We can bake all the processing into LUT, which is also practical for real-time rendering.

Make larger view frustum, and apply rotation at runtime.

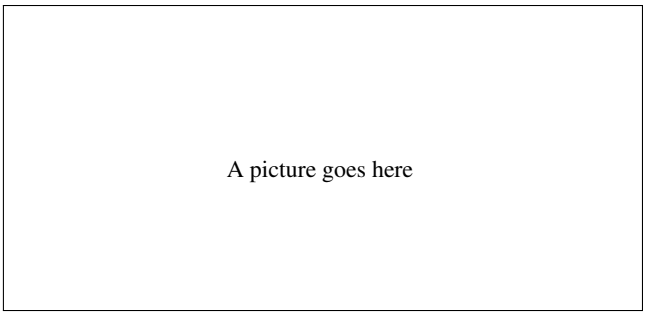

Figure 6: *[TODO] Draw an example of 1D glare (i.e., cross-section of superposition of 2D circles as boxcar functions).*

7.5 Motivation: Example by Time Complexity

Compare with the brute-force complexity and our approach.

[TODO] Key idea: per-pixel evaluation can avoid object dependency by aggregating the coefficients in preceding steps.

7.6 Extension to Non-Constant Functions

It might be better to choose non-square wave to better approximate non-square waves. One of the choices can be triangular waves with cosine-series expansion.

Radially Symmetric

Arbitrary Function (e.g., aperture ghost)

8 Associating with Matrix Optics

Now, we need to derive attributes of ghost a_k and b_k. We may apply ray tracing, but using 1D paraxial approximation is handy yet plausible approximation.

8.1 Enumeration of Even-Number Reflections

The previous studies used only single-pair reflections, but their ignorance has non-trivial effects in the veiling glare rendering. So, here we enumerate further reflections beyond degrees of 2 up to 4, 6, 8, ...

9 Postfiltering

Apply smoothing and fighting against ringing. We need to avoid ringing from low degrees.

Median blur could be good to avoid peak signals around edges; ringing typically happens around the edges of boxcar function.

10 Results

show effects of k, which sharpness control parameter.

show the out-of-screen synthesis and demonstrate in-screen synthesis. Then, verify the effectiveness of our strategy on periodic assumption.

11 Applications

11.1 Auto-driving vehicles

11.2 Glare Removal

12 Discussions and Limitations

Our approach only works for radially symmetric functions, which is the case for fully open aperture setting in optical systems

References

COZZI, F., ELIA, C., GEROSA, G., ROCCHETTA, F., LANARO, M., AND RIZZI, A. 2018. Use of an occlusion mask for veiling glare removal in hdr images. *Journal of Imaging 4*, 8, 100.

GU, J., RAMAMOORTHI, R., BELHUMEUR, P., AND NAYAR, S. 2009. Removing image artifacts due to dirty camera lenses and thin occluders. *ACM Transactions on Graphics (TOG) 28*, 5, 144.

KOREBAN, F., AND SCHECHNER, Y. Y. 2009. Geometry by deflaring. In *2009 IEEE International Conference on Computational Photography (ICCP)*, IEEE, 1–8.

NAYLOR, A. G. 1970. Veiling glare due to multiple reflections between surfaces. *Canadian Journal of Physics 48*, 22, 2720–2724.

RASKAR, R., AGRAWAL, A., WILSON, C. A., AND VEERARAGHAVAN, A. 2008. Glare aware photography: 4d ray sampling for reducing glare effects of camera lenses. *ACM Transactions on Graphics (TOG) 27*, 3, 56.

ROUF, M., MANTIUK, R., HEIDRICH, W., TRENTACOSTE, M., AND LAU, C. 2011. Glare encoding of high dynamic range images. In *CVPR 2011*, IEEE, 289–296.

SMITH, G. 1971. Veiling glare due to reflections from component surfaces: the paraxial approximation. *Optica Acta: International Journal of Optics 18*, 11, 815–827.

TALVALA, E.-V., ADAMS, A., HOROWITZ, M., AND LEVOY, M. 2007. Veiling glare in high dynamic range imaging. In *ACM Transactions on Graphics (TOG)*, vol. 26, ACM, 37.

WILLIAMS, T. 1998. *The optical transfer function of imaging systems*. CRC Press.